Neuro-Oncology Advances

3(1), 1–15, 2021 | https://doi.org/10.1093/noajnl/vdab175 | Advance Access date 22 November 2021

Involvement of platelet-derived VWF in metastatic growth of melanoma in the brain

Jose R. Robador[†], Manuel J. Feinauer[†], Stefan W. Schneider, Frank T. Mayer, Christian Gorzelanny, Artur Sacharow, Xiaobo Liu, Anna Berghoff, Maria A. Brehm, Daniela Hirsch, Julia Stadler, Sabine Vidal-y-Si, Ewa Wladykowski, Marisse Asong, Kai Nowak, Marcel Seiz-Rosenhagen, Viktor Umansky, Christian Mess, Klaus Pantel, Frank Winkler[†], and Alexander T. Bauer[†]

Department of Dermatology and Venereology, University Hospital Hamburg-Eppendorf, Hamburg, Germany (J.R.R., S.W.S., C.G., A.S., X.L., M.A.B., J.S., S.V., E.W., C.M., A.T.B.); Neurology Clinic and National Center for Tumor Diseases, University Hospital Heidelberg, Heidelberg, Germany (M.J.F., A.B., F.W.); Clinical Cooperation Unit Neurooncology, German Cancer Consortium (DKTK), German Cancer Research Center (DKFZ), Heidelberg, Germany (M.J.F., A.B., F.W.); Department of Dermatology and Venereology, Medical Faculty Mannheim, University of Heidelberg, Mannheim, Germany (F.T.M., V.U., A.T.B.); Institute of Pathology, University Medical Center Mannheim, Medical Faculty Mannheim, University of Heidelberg, Mannheim, Germany (D.H.); Division of Translational Cancer Research, Department of Laboratory Medicine, Lund University, Lund, Sweden (M.A.); Lund Stem Cell Center, Department of Laboratory Medicine, Lund University, Lund, Sweden (M.A.); Department of Surgery, RoMed Kliniken Klinkum Rosenheim, Rosenheim, Germany (K.N.); Department of Neurosurgery, Municipal Hospital Memmingen, Memmingen, Germany (M.S-.R.); Skin Cancer Unit, German Cancer Research Center (DKFZ), Heidelberg, Germany (V.U.); Department of Tumor Biology, University Medical Centre Hamburg-Eppendorf, Hamburg, Germany (K.P.)

[†]*Shared first, shared last.*

Corresponding Author: Alexander T. Bauer, Dr. sc. hum., Department of Dermatology and Venereology, University Hospital Hamburg-Eppendorf, Martinistraße 52, 20246 Hamburg, Germany (a.bauer@uke.de).

Abstract

Background. The prognosis of patients with brain metastases (BM) is poor despite advances in our understanding of the underlying pathophysiology. The high incidence of thrombotic complications defines tumor progression and the high mortality rate. We, therefore, postulated that von Willebrand factor (VWF) promotes BM via its ability to induce platelet aggregation and thrombosis.

Methods. We measured the abundance of VWF in the blood and intravascular platelet aggregates of patients with BM, and determined the specific contribution of endothelial and platelet-derived VWF using *in vitro* models and microfluidics. The relevance for the brain metastatic cascade *in vivo* was demonstrated in *ret* transgenic mice, which spontaneously develop BM, and by the intracardiac injection of melanoma cells.

Results. Higher levels of plasma VWF in patients with BM were associated with enhanced intraluminal VWF fiber formation and platelet aggregation in the metastatic tissue and peritumoral regions. Platelet activation triggered the formation of VWF multimers, promoting platelet aggregation and activation, in turn enhancing tumor invasiveness. The absence of VWF in platelets, or the blocking of platelet activation, abolished platelet aggregation, and reduced tumor cell transmigration. Anticoagulation and platelet inhibition consistently reduced the number of BM in preclinical animal models.

Conclusions. Our data indicate that platelet-derived VWF is involved in cerebral clot formation and in metastatic growth of melanoma in the brain. Targeting platelet activation with low-molecular-weight heparins represents a promising therapeutic approach to prevent melanoma BM.

© The Author(s) 2021. Published by Oxford University Press, the Society for Neuro-Oncology and the European Association of Neuro-Oncology. This is an Open Access article distributed under the terms of the Creative Commons Attribution-NonCommercial License (https://creativecommons.org/licenses/by-nc/4.0/), which permits non-commercial re-use, distribution, and reproduction in any medium, provided the original work is properly cited. For commercial re-use, please contact journals.permissions@oup.com

Key Points

- VWF secretion is associated with BM.
- VWF promotes platelet aggregation and BM.
- Anticoagulation with LMWHs might represent a novel target to reduce the occurrence of BM.

Importance of the Study

Brain metastases (BM) are associated with a high incidence of thrombotic complications, which define tumor progression and the high mortality rate. Cancer patients with BM thus belong to the highest risk group for the development of venous thrombosis, suggesting that coagulation drives tumor cell dissemination and brain colonization. Our study shows that von Willebrand factor promotes microthrombus formation and enhances BM formation. Importantly, low-molecular-weight heparins with dual functions on coagulation and on factors secreted by activated platelets, such as VEGF-A, significantly reduce the number of thrombotic vessel occlusions and BM. We have identified key mechanisms underlying the pathogenesis of BM, and propose platelet inhibition with low-molecular-weight heparins as a promising pharmacological intervention.

The incidence of brain metastases (BM) continues to increase despite the availability of improved treatment options for cancer patients.[1] Among solid tumors, the highest frequency of BM occurs in malignant melanoma, with up to 50% of all patients affected.[2] Severe neurological symptoms are associated with a strong negative effect on quality of life. BM requires tumor cells to cross the blood-brain barrier (BBB), a tight structural barrier consisting of endothelial cells (ECs), pericytes, and astrocytic endfeet, which limits the passage of compounds and maintains brain homeostasis.[2] A major challenge hindering the development of effective therapies is our limited understanding of the molecular interactions between tumor cells and the BBB within the brain metastatic cascade.[3]

Cancer-associated thrombosis (CAT) is a common complication in patients with malignancies and the risk is particularly high in melanoma patients with BM.[4] Furthermore, the incidence of stroke is usually associated with occult and manifested cancer, and negatively correlates with the patient's prognosis and outcome.[5] Several candidates that may promote CAT and metastasis have been identified recently, including von Willebrand factor (VWF), a glycoprotein involved in hemostasis.[6,7] VWF is stored in platelets and ECs, and its secretion into the plasma is triggered by multiple stimuli.[8] Importantly, VWF levels increase in the plasma of melanoma patients, associated with luminal VWF network formation and thrombotic vessel occlusions in tumor specimens.[9] Preclinical data based on a mouse model characterized by long-lasting VWF fibers due to a missing VWF degrading enzyme "a disintegrin and metalloprotease with a thrombospondin type 1 motif, member 13" (ADAMTS13), revealed abnormal intravascular platelet accumulation leading to lung metastases.[10] Notably, the observation that a local primary skin melanoma promotes luminal VWF fibers and platelet aggregation in distant organs such as the liver, lung, and brain may indicate that VWF is a trigger for CAT and BM.[10] Accordingly, we recently used *in vivo* imaging to demonstrate that intravascular clots and VWF deposition promote tumor cell arrest and extravasation in a mouse model, which could be blocked by the antibody-mediated inhibition of VWF.[11] However, the precise mechanisms of VWF deposition and platelet activation, and their relevance in the context of human disease, remain unknown.

Here we investigated mechanisms by which VWF influences vessel occlusions within brain capillaries and BM in mice and humans. The contribution of VWF to the pathogenesis of BM was determined using human blood and brain metastatic tissue samples, and the molecular mechanisms were investigated *in vitro* using microfluidics, and in mouse models of melanoma BM.

Methods

See also Supplementary Methods.

Patient Materials

We analyzed tissue from seven BM along with the perimetastatic regions in the resection margin, defined by experienced pathologists as the brain tissue surrounding the macroscopic metastases but separated from them by 1–2 mm. VWF concentrations and ADAMTS13 activity was measured in citrated plasma[9] from 38 metastatic melanoma patients (14 with BM) at Universitätsklinikum Eppendorf, Hamburg, Germany. All patients provided informed consent,

which was approved by the ethical commissions of the Hamburger Ärztekammer (PV3779, PV5392). As inclusion criteria, subjects were required to be at least 18 years old with a confirmed diagnosis of stage IV melanoma, no specific melanoma therapy during the previous 4 weeks, and at least 6 months of clinical follow-up. We also included 11 control patients with semi-malignant basal cell carcinoma (BCC).

Animal Experiments

All animal procedures were approved by the governmental animal care authorities (Regierungspräsidium Karlsruhe). The *ret* transgenic mice[12] were treated with 0.6 IU/g tinzaparin (Innohep; Leo Pharma, Germany) subcutaneously as previously described.[9] For intracardiac tumor cell injections, 5×10^5 A2058 cells in 100 µL phosphate-buffered saline were introduced into male Naval Medical Research Institute (NMRI)-nu mice at 8–12 weeks of age (Charles River) as previously described.[13]

Immunohistochemistry

We prepared 10-µm coronal cryosections and stained those spaced at least 130 µm apart to avoid the extensive overlap of metastases in serial sections. BM were quantified by hematoxylin and eosin (H&E) staining. Bright-field images were acquired using an Axio Scan. Z1 slide scanner (Carl Zeiss) fitted with a 20×/0.8 Plan-Apochromat objective (Carl Zeiss) and an HV-F202SCL camera (Hitachi, Japan), or with a digital microscope and M8 scanner (PreciPoint).

Immunofluorescence Analysis

Immunostaining was performed using the following primary antibodies: rabbit anti-human VWF (1:150; Dako), mouse anti-Human TSP (1:75, Laboratory Vision/Neomarkers) rat anti-mouse CD31 (1:50; BD Biosciences), rat anti-mouse GPIbα/CD42 (1:100; EMFRET Analytics), mouse anti-human CD31 (1:50; Dako), and rabbit anti-mouse vascular endothelial growth factor-A (VEGF-A) (1:150; Santa Cruz). Following secondary antibodies were used: fluorescein isothiocyanate (FITC)-conjugated goat anti-rabbit IgG (1:200; BD Pharmingen), Alexa 555-conjugated goat anti-rat IgG (1:200; Invitrogen). Nuclei were counterstained with DAPI (1:1000). Fluorescence images were acquired with a Zeiss Axiovert 200 microscope and were analyzed using AxioVision v4.8 (Zeiss) and ImageJ v1.47c.

ELISA

VWF secretion was quantified by ELISA as previously described.[10] Briefly, ECs were stimulated with 4-(2-hydroxyethyl)-1-piperazineethanesulfonic acid (HEPES) buffered Ringer's solution, Thrombin (0.5 IU/mL), Trap-6 (10 or 50 µM), VEGF-A (2.5 ng/mL), collagen I (50 µg/mL), melanoma-derived supernatant alone or combined with tinzaparin (100 IU/mL), fondaparinux (50 µg/mL), or bevacizumab (0.65 mg/mL).

In situ Fibrinogen Binding

Coronal brain cryosections (10 µm) were incubated with 20 µg/mL Alexa 488-conjugated fibrinogen (Thermo Fisher Scientific) for 2 h before fixing in 4% paraformaldehyde. Platelets were stained using rat anti-mouse GPIbα (1:100) and Alexa 555-conjugated goat anti-rat IgG. Nuclei were counterstained with DAPI (1:1000).

Microfluidics

We cultured bEnd3 cells on a µ-Slide $I^{0.2}$ Luer IBIDI-slide (IBIDI) and perfused them at 2.5 dyne/cm^2 with isolated platelets and a hematocrit of 25% in HEPES-buffered saline using the IBIDI system as previously described.[14] Platelets from wild-type (Wt) and VWF$^{-/-}$ mice were labeled using Celltrace Orange AM (1:1000; Invitrogen). ECs were first stimulated with 100 µM histamine. We then activated the platelets by adding 50 µg/mL collagen type I and simultaneously added a FITC-conjugated anti-mouse VWF antibody (1:100; GeneTex).

Light Transmission Aggregometry

Platelet suspensions were recalcified using 1 mM $CaCl_2$ before adding 50 µg/mL collagen type I and preincubating for 30 min with tinzaparin (100 IU/mL) or fondaparinux (50 µg/mL). The suspensions were then analyzed by light transmission aggregometry (LTA) using a Model 700 device (Chrono-log).

Platelet Releasates

Platelets were exposed to collagen type I (50 µg/mL) for 15 min. Then, prostaglandin-E1 (1:1000) was added to stop the reaction. The releasate was collected by centrifugation (1200 g, 15 min RT). To test the effect of anticoagulant drugs on platelet releasate, platelets were preincubated with tinzaparin (100 IU/mL), fondaparinux (50 µg/mL), or bevacizumab (0.65 mg/mL) 30 min before activation. The Quantikine ELISA kit (R&D Systems) was used to quantify VEGF-A in platelet releasates.

Transmigration Assay

Human brain microvascular endothelial cells (HBMECs) were cultured on cell culture inserts with 8-µm pores (Millipore) coated in gelatin (Sigma-Aldrich). The inserts were transferred to 24-well plates and incubated at 37°C in a 5% CO_2 atmosphere until they reached confluency. We then added 2×10^4 *Ret* melanoma cells labeled with Celltrace Orange AM (1:1000) and 200 µl of human platelet releasate with or without additives. Melanoma cells were supplemented with releasate of resting platelets and activated platelets with or without tinzaparin (100 IU/mL) or bevacizumab (0.65 mg/mL). Tumor cell transmigration was counted 24 h later.

Statistical Analysis

Data are presented as means ± standard deviations calculated using GraphPad Prism v8.1.0 (GraphPad Software). A two-tailed Student's *t*-test was used to compare two

groups, and two-way ANOVA with Bonferroni correction was used to compare multiple groups. An *F*-test was used to analyze differences between linear results. Differences were considered statistically significant at $*P < .05$ and $**P < .01$.

Results

von Willebrand Factor Fibers Promote Platelet Clustering in Human Brain Metastases

To investigate the potential role of VWF in BM, we evaluated VWF in the intra- and perimetastatic regions of human brains by immunofluorescence microscopy (Figure 1A–D). Intraluminal VWF fibers were observed in all BM (Figure 1A and B) and in the corresponding perimetastatic regions (Figure 1C and D). When stretched, VWF fibers bind to circulating platelets.[6] Accordingly, all specimens were positive for intravascular platelet-rich thrombi (Figure 1A–D). To determine whether the formation of VWF fibers in BM is associated with higher plasmatic VWF and/or slower degradation, we measured VWF and ADAMTS13 activity in the peripheral blood of 38 malignant melanoma patients with advanced metastatic disease (including 14 patients with BM) and 11 controls with non-metastatic BCC. The serum VWF levels were significantly higher in patients with metastatic melanoma compared to BCC controls (Figure 1E). This correlated with a significant 20% reduction in ADAMTS13 activity (Figure 1F). Importantly, serum VWF levels were even higher in patients with diagnosed BM (Figure 1G) without further changes in ADAMTS13 activity (Figure 1H).

Cerebral Endothelial Cells Express Low Levels of von Willebrand Factor

VWF secreted by activated ECs promotes vessel occlusions,[6,8] but most *in vitro* data are based on primary macrovascular ECs of veins (HUVECs). Given that the amount of VWF produced by ECs varies according to the tissue of origin,[15] we focused on the microvascular endothelium of the brain. We compared the abundance of VWF in primary HBMECs and HUVECs by immunofluorescence microscopy. The transmembrane EC marker CD31 was distributed similarly in both cases and restricted to cell–cell contacts, but we observed the typical punctate distribution of VWF in the cytoplasm (Figure 2). However, whereas VWF was detected in most of the HUVECs (76.80 ± 19.55%), it was detected in only 26 ± 3.12% of the HBMECs (Figure 2A–C). Furthermore, the HBMECs accumulated significantly lower quantities of VWF (Figure 2B and D). This was also observed in murine microvascular brain ECs, represented by the bEND3 cell line (Supplementary Figure 1). We also analyzed the *in vivo* distribution of VWF in Wt mouse brains. Different groups of blood vessels were defined by their diameter: (a) < 10 μm, (b) 10–50 μm, and (c) > 50 μm (Figure 2E and F). Vessels with a small diameter (< 10 μm) contained significantly lower levels of VWF than wider blood vessels (Figure 2F).

Low von Willebrand Factor Secretion in Cerebral Endothelial Cells

Tumor cell-derived thrombin generation and VEGF-A can induce the activation of HUVECs and VWF secretion.[9] To determine whether the same mechanisms induce the activation of the brain microvascular endothelium, HBMECs, and bEnd3 cells were stimulated with a melanoma supernatant containing VEGF-A. The supernatant induced the formation of VWF fibers in all cases (Figure 3A–D, Supplementary Figure 1) and VWF secretion increased approximately 2.5-fold in HUVECs (Figure 3E). Melanoma cells can activate ECs directly via interaction or by secreted factors (Supplementary Figure 2). To determine the mechanisms of tumor cell-mediated EC activation, HUVECs, HBMECs, and bEnd3 were used. Melanoma cell supernatant and VEGF-A induced VWF release from HUVECs, HBMECs, and bEnd3, whereas VEGF-A inhibition with bevacizumab blocked VWF secretion in all cells (Figure 3E, Supplementary Figure 2). Likewise, HUVECs secreted similar levels of VWF following PAR-1 activation with thrombin or Trap-6 (Figure 3E, Supplementary Figure 2). By contrast, thrombin and Trap-6 failed to activate HBMECs and bEnd3 cells (Figure 3E, Supplementary Figure 2). This was supported by qPCR results (Supplementary Methods) confirming enhanced expression of VEGF receptor 2 (VEGF-R2) in HBMECs and the downregulation of PAR-1 compared to HUVECs (Figure 3F). Low VWF levels combined with the inability of thrombin to promote VWF secretion supports the tissue-specific regulation of VWF in the brain.

Brain Metastases Are Associated With von Willebrand Factor Fibers

We used the *ret* transgenic mouse model that spontaneously develops melanoma with metastases in the lymph nodes, lungs, and brain (Figure 4A). The histopathology of BM in this model resembles that in human melanoma patients.[12] Immunohistochemical analysis revealed macroscopic metastatic brain lesions in approximately 30% of the mice (Figure 4B). VWF stored in the endothelium showed a punctuate distribution in healthy Wt mice, and very few VWF fibers were detected in the vessel lumen, which is typical for nonactivated ECs (Figure 4C, lower left insert). In contrast, VWF networks were visible in the vessels of metastatic brain tissue and perimetastatic regions (Figure 4C, right inserts). For quantification, we defined four groups of interest: (a) healthy Wt brain, (b) cerebral tissue from tumor-bearing mice lacking macroscopically detectable BM (Met-Free), (c) peritumoral brain regions (Peri-Met), and (d) metastatic brain tissue (Intra-Met). VWF fibers were detected in only 22% of the Wt brain vessels, compared to 40% in Intra-Met (Figure 4D). Importantly, VWF networks increased to the same extent in vessels of Peri-Met and even in Met-Free brains (Figure 4D).

To determine the relative contribution of endothelial versus platelet-derived VWF, we quantified the fractions of VWF stored in the vessel wall and lumen. In healthy skin, used as control for quiescent endothelium, the VWF signal in the lumen ($VWF_{luminal}$) was negligible but the VWF signal within the vessel wall ($VWF_{endothelial}$) was strong (Figure 4E

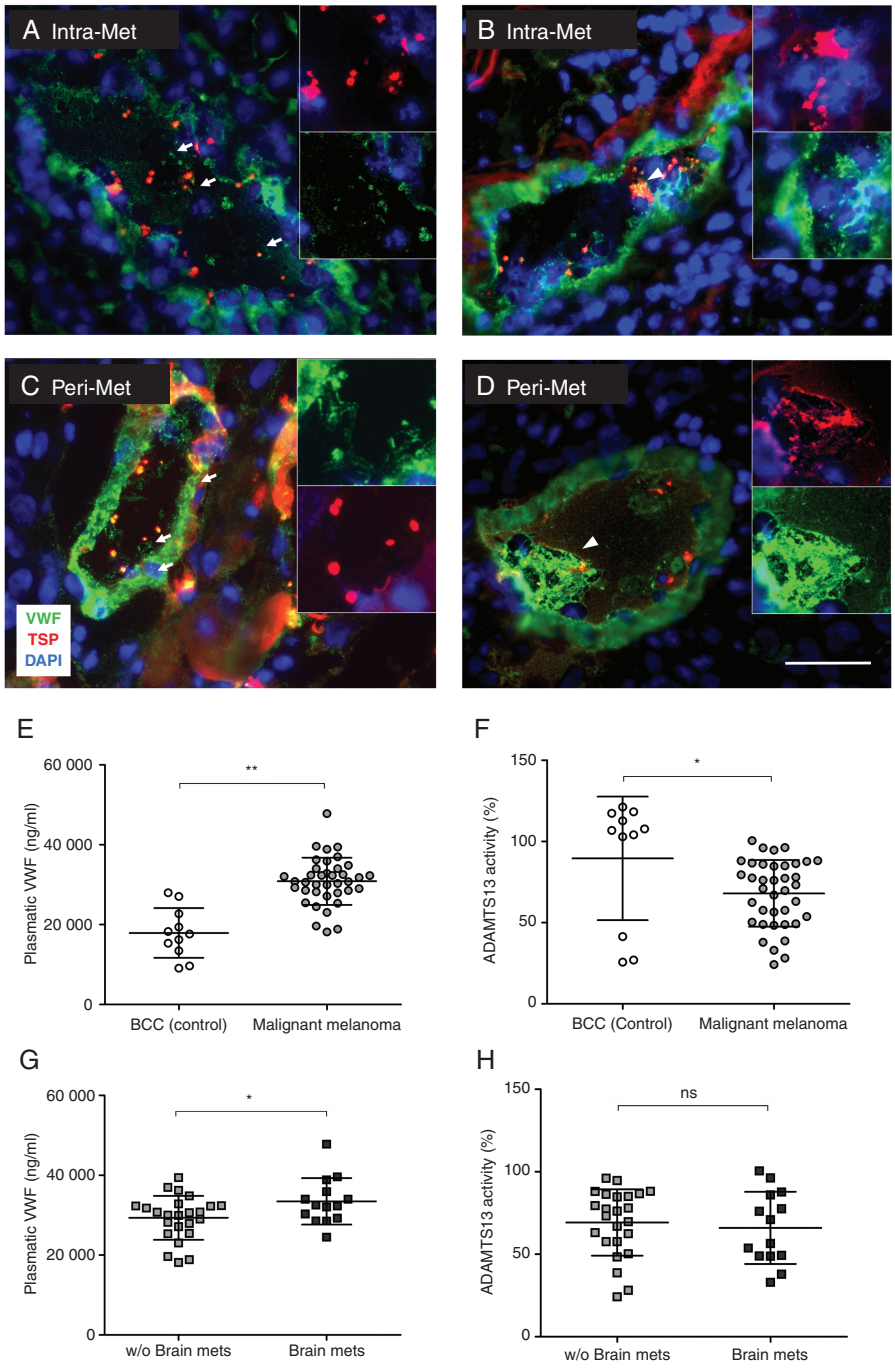

Figure 1. Luminal VWF fibers and platelet aggregates are detected in the brain vessels of patients with BM. Immunofluorescence staining of VWF and platelet TSP shows luminal VWF fibers (arrows) and platelet aggregates (arrowheads) in Intra-Met (A, B) and Peri-Met (C, D) cerebral tissue from patients with BM ($n = 7$ patients). (E–H) VWF concentration and ADAMTS13 activity were measured in the plasma of BBC patients, used as control for non-metastatic skin tumor, and malignant melanoma patients with or without BM ($n \geq 11$ patients/group). Ns = not significant, $^{*}P < .05$, $^{**}P < .01$, scale bar 50 μm.

and F). In contrast, vessels in primary skin tumors were characterized by EC activation, including pronounced luminal VWF networks ($VWF_{luminal}$) combined with reduced VWF levels in the vessel wall ($VWF_{endothelial}$) confirming EC-derived VWF secretion (Figure 4E and F). In healthy Wt brains, we detected VWF stored in the vessel wall but no luminal VWF fibers, indicating the absence of EC-related VWF fiber secretion (Figure 4F). In contrast, we observed

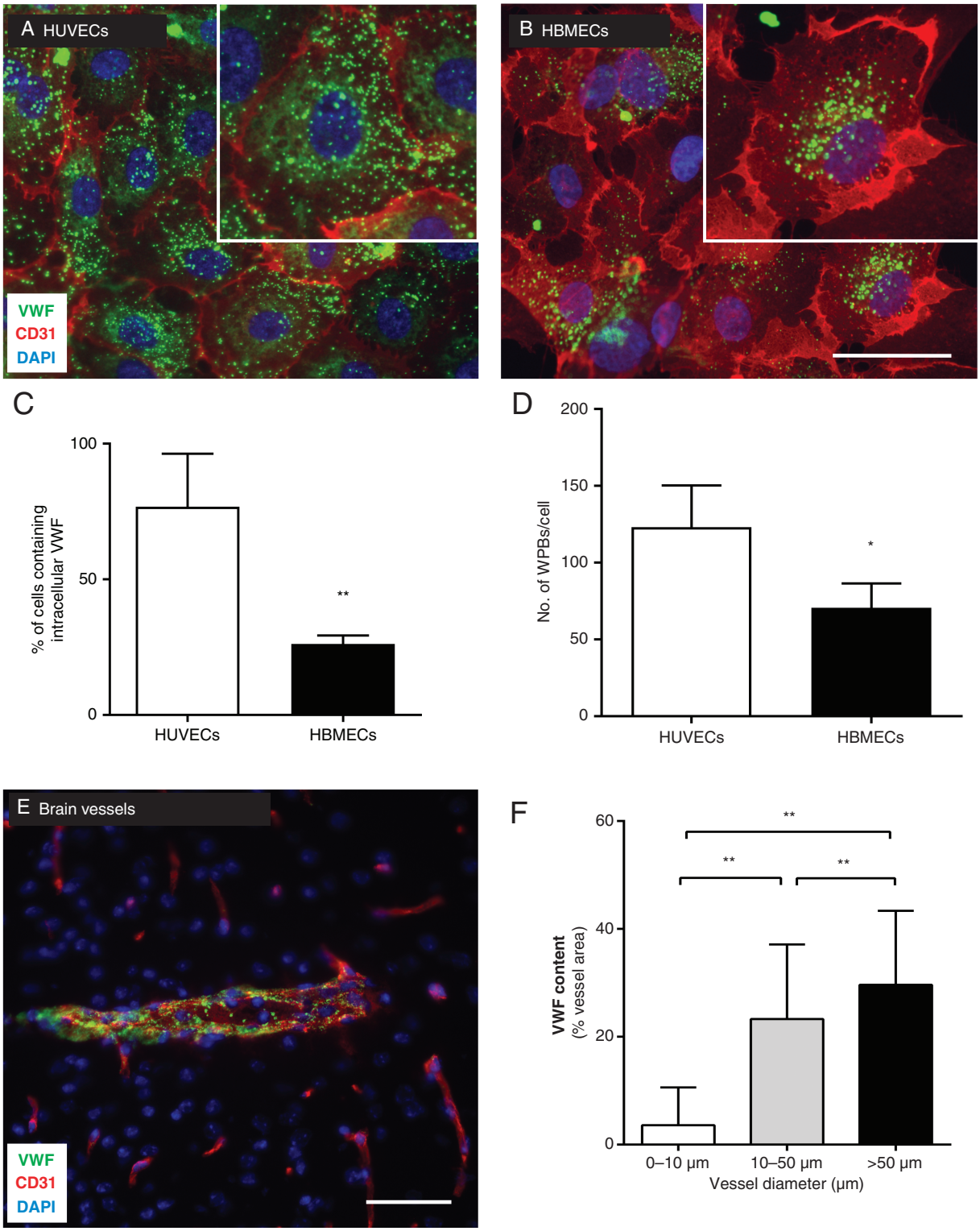

Figure 2. Distribution of VWF in the brain microvasculature is heterogeneous. Immunofluorescence staining of VWF and CD31 shows the distribution of VWF in HUVECs (A) and HBMECs (B). The number of cells expressing VWF (C) and the number of VWF storage granules per cell (D) were quantified in both cell types (n = 1,000–2,000 cells/group). (E) Sections of Wt brains were stained for VWF and CD31, and (F) cerebral vessels were grouped by their diameter and VWF content (n = 504 vessels). *P < .05, **P < .01, scale bar 50 µm.

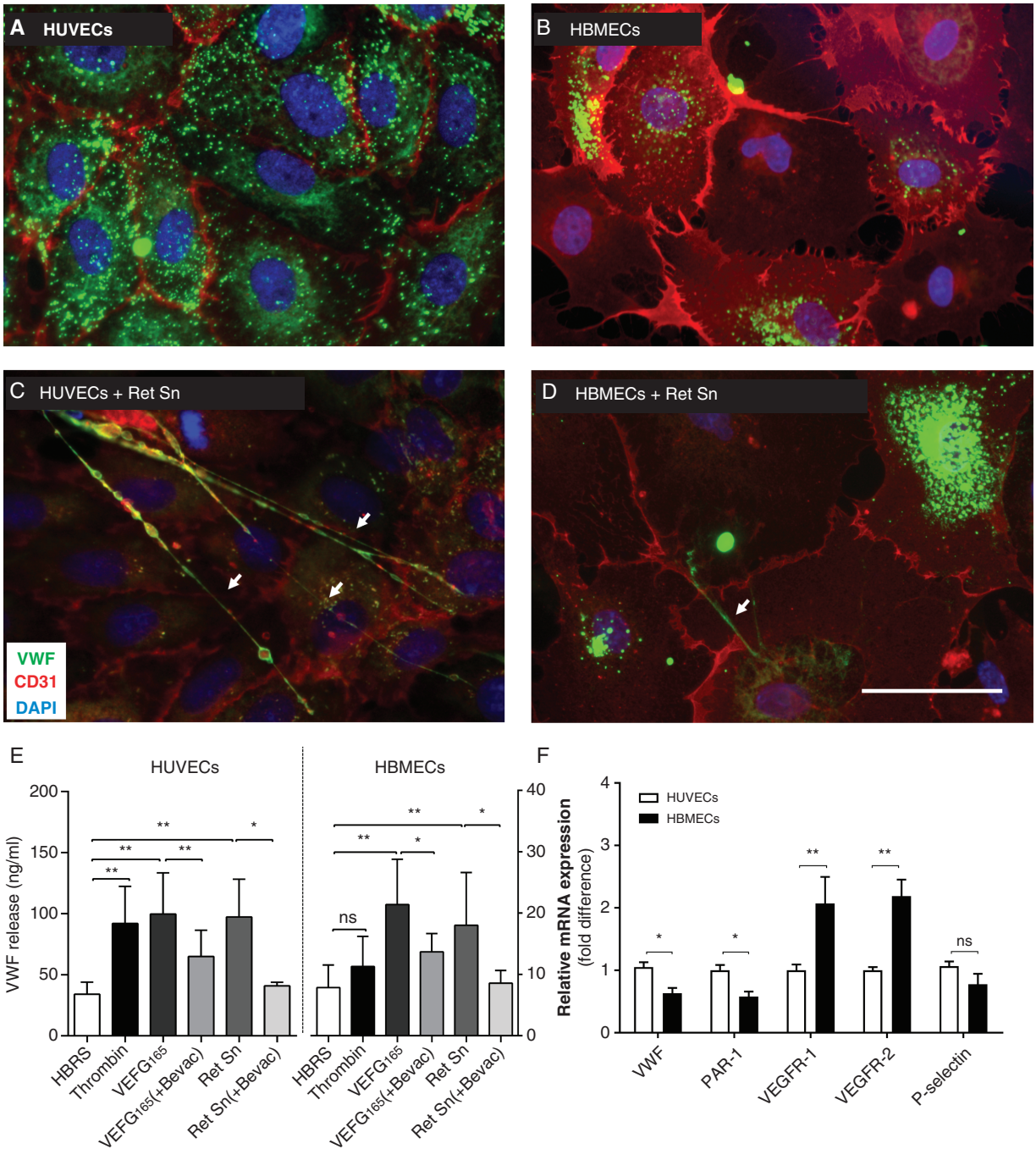

Figure 3. Brain microvascular endothelial cells show a limited release of VWF. Representative images of quiescent HUVECs (A) and HBMECs (B) show intracellular stored VWF. Incubation with the supernatant of *Ret* melanoma cells (Ret Sn) triggers the release of VWF and the formation of luminal VWF fibers (arrows) (C, D). Activation of HUVECs and HBMECs was induced using different stimuli and the secretion of VWF was measured in the supernatant ($n \geq 3$ experiments/group). (F) The expression of P-selectin, VWF, PAR-1, VEGFR-1, and VEGFR-2 was examined in HUVECs and HBMECs by qPCR ($n = 3$ experiment). Ns = not significant, $^{*}P < .05$, $^{**}P < .01$, scale bar 50 μm.

an increase in luminal VWF networks ($VWF_{luminal}$) in the vessels of metastatic brain tissues correlating with the depletion of VWF stored in the vessel wall ($VWF_{endothelial}$). This reflects the activation of ECs and the secretion of VWF into the lumen (Figure 4F). Surprisingly, in Peri-Met and Met-Free brains of mice with multiple skin tumors, we detected a significant increase in the abundance of VWF fibers without marked loss of $VWF_{endothelial}$ (Figure 4F) indicating no significant change in $VWF_{endothelial}$. Therefore, VWF secretion by ECs may not be completely responsible

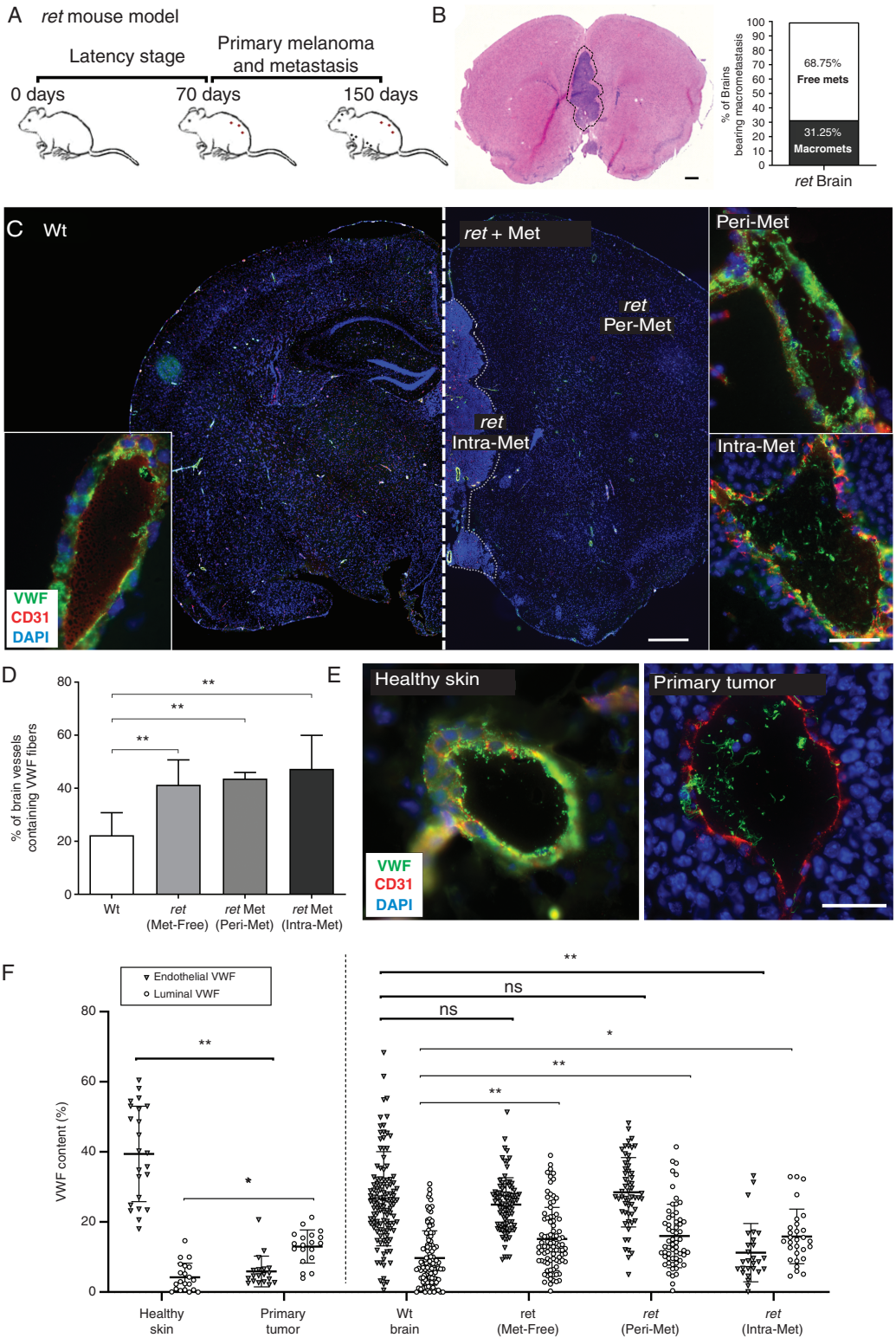

Figure 4. Luminal VWF fibers are associated with melanoma brain metastasis. (A) The *ret* mouse, characterized by spontaneous melanoma development and BMs. (B) BMs (dashed line) were detected by immunohistochemical staining ($n = 40$) and *ret* brains were divided into three groups: Met-free, Peri-Met, and Intra-Met. (C) Wt and *ret* brain cryosections were stained for VWF and CD31, and (D) the percentage of cerebral vessels containing luminal VWF fibers was calculated ($n = 4$–6 brains/group). Endothelial cell activation and VWF release was defined by measuring the fractions of VWF in the vessel wall and vessel lumen. (E) Skin vessels and melanoma primary tumor vessels were used as controls for quiescent and activated endothelium, respectively. (F) VWF stored in the vessel wall and in the vessel lumen was quantified ($n = 20$–117 vessels/group). Ns = not significant, $^*P < .05$, $^{**}P < .01$, scale bar 50 μm.

for the observed VWF fibers and platelet-derived VWF may contribute to luminal VWF network formation.

Platelets Secrete VWF Fibers During the Formation of Brain Metastases

Given the abundance of VWF in platelets, we explored platelet activation and VWF multimer release in BM. Fibrin promotes platelet binding and activation[16] so we used an *in situ* fibrinogen binding assay (Figure 5). Platelets in Wt brains were characterized by a low fibrinogen-CD42 colocalization (Figure 5A and B). In contrast, cerebral vessels of ret mice exhibited a strong increase of fibrinogen–CD42 colocalization (Figure 5A and B). Unlike the discoid-like resting platelets within Wt brains, these activated thrombocytes changed to a more spherical form, projected pseudopodia and released VWF, which assembled to form long VWF strings on the platelet surface (Figure 5C). Accordingly, platelet activation correlated with a significant increase in thrombocyte aggregation (Figure 5D, Supplementary Figure 3). Interestingly, the number of platelet aggregates/vessel in Met-free tissue and Intra-Met vasculature was not different (Figure 5D) suggesting that platelet activation and aggregations did not differ between ret brains with and without metastases. Next, we investigated whether the LMWH tinzaparin could suppress platelet activation and aggregation in the cerebral microvasculature. We found that prolonged treatment with tinzaparin (0.6 IU/g daily for 100 days) abolished platelet–fibrinogen colocalization (Figure 5B). This correlated with VWF stored within platelets, fewer secreted VWF strings, and with less intravascular thrombocyte aggregation (Figure 5D). These findings were verified in a second mouse model, based on the intracardiac injection of A2058 melanoma cells (Supplementary Figure 4).

von Willebrand Factor Promotes Microthrombus Formation

To unravel the role of VWF in thrombocyte deposition and aggregation on an endothelial monolayer, unidirectional shear stress was applied using an IBIDI pump. Platelets isolated from Wt and VWF$^{-/-}$ mice were added to the system. In the first step, the addition of histamine triggering EC activation without affecting the thrombocytes (Supplementary Figure 5) resulted in the formation of short platelet strings on the surface of bEnd3 cells (Figure 5E). Quantification revealed no significant differences in the deposition of VWF$^{-/-}$ platelets and Wt thrombocytes (Figure 5F). We then added collagen type I, which stimulates platelets followed by VWF secretion without affecting ECs (Supplementary Figure 5). Microaggregation on the luminal surface of ECs appeared to be more pronounced in Wt platelets than in VWF-/- platelets (Video 1 and Video 2). Quantification revealed a surface coverage of 311.55 ± 121.32 µm^2 with Wt platelets but only 74.59 ± 42.51 µm^2 with VWF-deficient thrombocytes (Figure 5F). Finally, LTA showed that VWF$^{-/-}$ platelets significantly reduced aggregation by 12.28% (Figure 5G) demonstrating that microthrombus formation is actively fostered by platelet-derived VWF.

Anticoagulation Attenuates Brain Metastases

Because we hypothesized that platelets contribute to BM, we analyzed platelet activation and aggregation by LTA (Figure 6A) and by measuring VEGF-A in the platelet releasate (Figure 6B). Platelet aggregation induced by thrombin and collagen type I was associated with high levels of VEGF-A. In contrast to fondaparinux, preincubation of thrombocytes with tinzaparin blocked platelet aggregation and reduced VEGF-A secretion (Figure 6A and B). Fondaparinux exerts its anticoagulant activities primarily by inhibition of factor Xa. Tinzaparin inhibits factor Xa and factor IIa. Therefore, heparins block the activation of thrombin, a process that requires plasmatic coagulation factors.[17] We could previously show that in contrast to fondaparinux, tinzaparin has a strong binding affinity to VEGF-A. In the absence of coagulation factors, tinzaparin blocks platelet aggregation via VEGF-A binding and inhibition, whereas fondaparinux lacks the capacity to suppress VEGF-A.[9] In line, transmigration assays showed that the releasates from activated human platelets increased the transmigration of melanoma cells more effectively than releasates from resting platelets (Figure 6C and D). Addition of tinzaparin and the VEGF-A neutralizing antibody bevacizumab to prestimulated platelets blocked platelet-induced invasion of melanoma cells (Figure 6C and D). Furthermore, electric cell-substrate impedance spectroscopy (ECIS) revealed that bevacizumab and tinzaparin reversed platelet-induced changes of the endothelial integrity (Supplementary Figure 6). Platelets also store transforming growth factor (TGF)-β with a heparin binding domain.[18] However, TGF-β did not affect tumor cell transmigration (Supplementary Figure 7). We next assessed the distribution of VEGF-A in *ret* transgenic mice. Metastatic brain tissue (Intra-Met) exhibited strong VEGF-A expression, but only low levels were detected in healthy Wt and perimetastatic (Peri-Met) tissue (Supplementary Figure 8A and B). Importantly, an increase of luminal VEGF-A and platelet coverage in Intra-Met and Peri-Met vessels was abolished by tinzaparin treatment (Supplementary Figure 8C and H).

For an *in vivo* proof, we injected mice intracardially with A2058 melanoma cells. Tinzaparin treatment (0.6 IU/g) was started 2 days before the injection and continued daily until day 10 (Figure 6E). On day 28, metastatic lesions in the brain were analyzed by H&E staining of coronal sections (Figure 6F). We found that tinzaparin significantly reduced the brain metastatic load (Figure 6G and H). In summary, our results show that VWF promotes intracerebral platelet aggregation, platelet activation, and BM. Anticoagulation with tinzaparin prevents BM and provides novel insights into the underlying pathophysiological mechanism that may facilitate the development of new therapeutic strategies (Figure 6I).

Discussion

Because the occurrence of BM is a leading cause for a very poor prognosis and severe neurological symptoms, there is an urgent need for the prevention and treatment

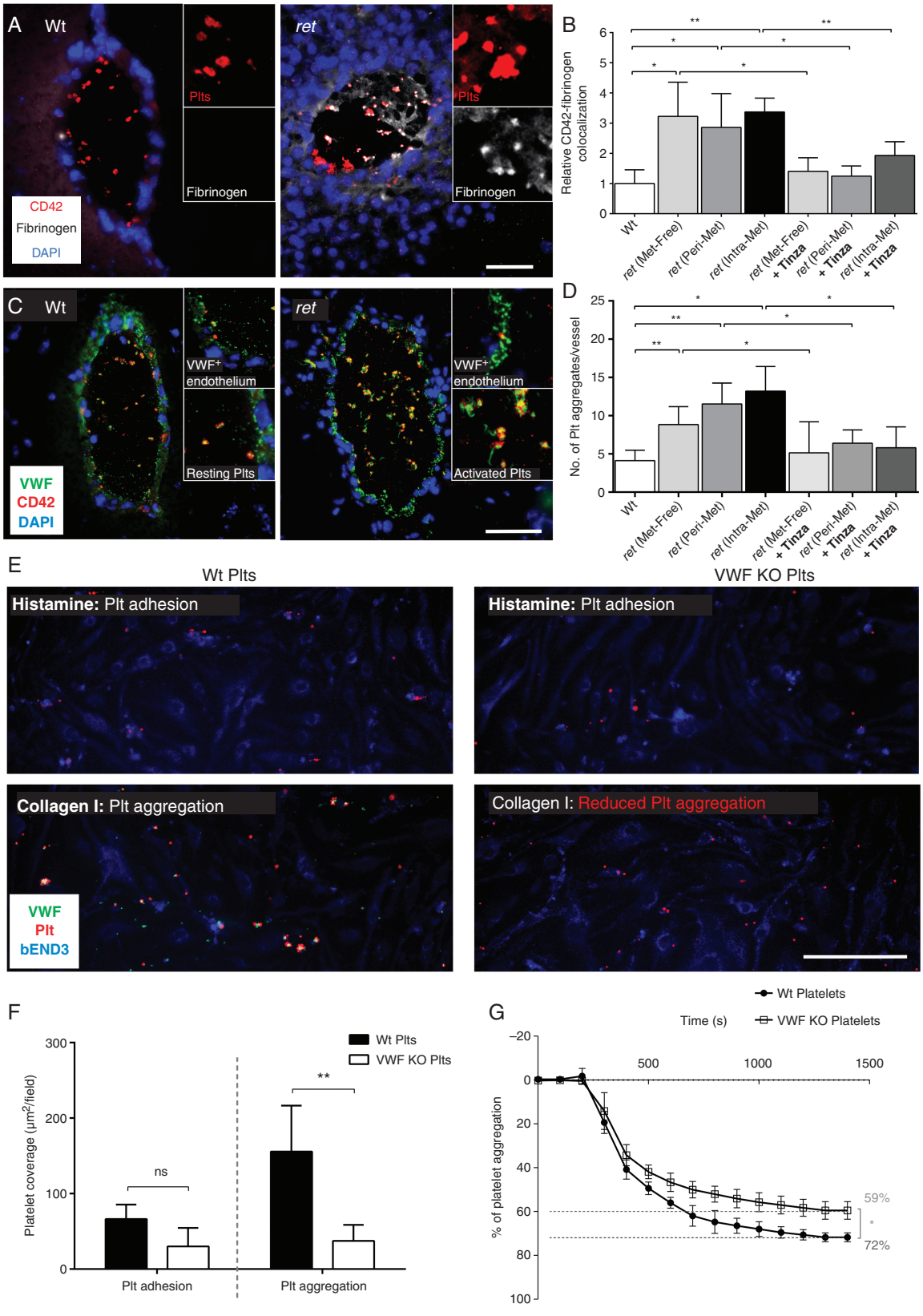

Figure 5. VWF promotes the aggregation of platelets. (A) *In situ* fibrinogen binding assay and immunofluorescence staining of CD42 were combined to identify activated platelets in brain tissue. (B) Manders' colocalization coefficient was calculated to analyze the interaction between

of brain metastases. However, an understanding of the molecular mechanisms underlying the brain metastatic cascade lags far behind that of other aspects of tumor progression. Own studies based on an *in vivo* model recently showed that VWF promotes intravascular clotting and tumor cell extravasation into the brain.[11] While these data provide clear evidence for a role of VWF in the brain metastatic cascade, it remains elusive how VWF promotes BM.

The aim of this study was to identify the mechanisms of VWF-mediated coagulation and its impact on BM. We found that VWF fibers secreted by activated platelets may be involved in brain metastasis formation. Another critical step was that platelet-derived VWF in turn provokes platelet activation and clotting. Therefore, VWF represents a significant mechanism for intracerebral hypercoagulation and BM.

The functional relevance of VWF in the brain was demonstrated in a mouse model of allergic encephalomyelitis. BBB permeability was increased and the disease outcome was more severe in VWF-deficient mice compared to Wt, suggesting that VWF reduces BBB permeability.[19] In contrast, the analysis of mouse models of hypoxia/reoxygenation, pilocarpine-induced status epilepticus,[20] ischemic stroke,[21–23] and cerebral malaria[24] indicate that VWF increases the permeability of the BBB. The latter is not unexpected in the context of coagulation and inflammation, given the ability of VWF secreted by ECs to recruit circulating platelets, and leukocytes.[6,25] Moreover, VWF secretion from activated ECs promotes thrombotic vessel occlusions and metastases.[9,10] However, these studies missed that VWF is also stored in platelets and the functional differences between the two VWF pools are not yet clear.

The role of EC-derived VWF in atherosclerosis was suggested by the inability of platelet-derived VWF to trigger atherosclerotic plaque formation in chimeric mice generated by bone marrow transplantation.[26] In a similar mouse model, platelet-derived VWF was unable to support arterial thrombus formation following $FeCl_3$-induced carotid artery occlusion, and chimeric mice with VWF solely in platelets exhibited normal bleeding times.[27] Interestingly, the same study demonstrated that platelet-derived VWF seems to trigger cerebral infarctions in ischemic stroke,[27] which is supported by experiments showing the role of platelets in the modulation of cerebral bleeding.[28] Indeed, the low levels of VWF and the restricted secretion in brain ECs may explain the relevance of platelet-derived VWF in the central nervous system. Low VWF levels in cerebral capillaries may define regulated transport processes, whereas the abundant VWF in venules promotes leukocyte transmigration during inflammation.[29] Notably, we showed that downregulation of the thrombin receptor (PAR-1) attenuates thrombin-mediated VWF secretion in brain ECs. This may be specific to the brain, because the low concentrations of tissue factor pathway inhibitor and high levels of thrombin in the brain would support diffuse thrombotic complications.[30]

Supported by clinical observations,[7,31] our data indicate that the elevation of VWF in melanoma patients with BM triggers uncontrolled platelet aggregation, defining the high risk for CAT.[4] We also observed increased platelet activation, indicating that platelet-derived VWF could trigger intracerebral thrombosis and metastasis. In line with previous studies in patients with malignant brain tumors,[32] we detected a mild reduction of ADAMTS13 activity in melanoma patients with BM that should not affect the degradation of luminal VWF multimers.[33–35] A differential glycosylation of platelet-derived VWF, which provides specific resistance against cleavage,[36,37] may explain the observed VWF strings in brain metastatic tissue. We used VWF-deficient mouse platelets to show the impact on platelet aggregation. Accordingly, as well as binding to collagen,[38] platelet-derived VWF strings could help to recruit new circulating platelets.[37,39] Our data indicate that platelet-derived VWF could be relevant for metastatic growth of melanoma in the brain via a local increase of platelet-derived molecules such as VEGF-A. Indeed, VEGF-A was shown to be overexpressed in melanoma and associated with poorer outcome.[40,41] It is therefore likely that VEGF is involved in the brain metastatic cascade. However, anti-VEGF-A strategies have no clinical role in the treatment of melanoma. Bevacizumab treatment following surgical resection in melanoma patients did not improve overall survival of the included patients.[42] It is important to mention that although VEGF-A affects multiple steps of the metastatic cascade,[43–46] a vast amount of molecules is involved in BM formation.[47] Next to VEGF, the involvement of heparanase, TGF-β, and selectins has been proposed.[48,49] To simultaneously inhibit several molecules involved in thrombosis and metastasis, we evaluated the therapeutic effect of the LMWH tinzaparin. Heparins consist of a complex mixture of natural glycosaminoglycans responsible for the binding to large number of molecules. Next to its anticoagulant activity, tinzaparin exerts its anti-metastatic activity via binding and inhibition of distinct molecules involved in the extravasation of tumor cells, such as VEGF-A,[9] heparanase, and selectins.[50] Since our data demonstrate a clear therapeutic effect of tinzaparin, LMWHs may represent antithrombotic and innovative therapeutic targets for cancer treatment.

However, clinical studies evaluating LMWH in cancer patients provided modest results. Only few clinical trials reported a significant survival benefit in cancer patients receiving LMWHs.[51] In addition, the FAMOUS study demonstrated no impact of dalteparin on survival

Fibrinogen and CD42. Results were normalized to the mean value observed in Wt brains (n = 4–6 brains/group). (C) Immunofluorescence staining of VWF and CD42 showed platelet-derived VWF secretion correlating with platelet aggregates. (D) The number of aggregates per vessel was quantified in each group (n = 4–6 brains/group). (E) Murine bEND3 cells were perfused with platelets isolated from Wt or VWF knockout (VWF KO) mice. (F) Platelet coverage was quantified before stimulation (Plt adhesion) and after activation (Plt aggregation) (n = 4–6 brains/group). (G) Distinct capacity of Wt and VWF KO platelets to form aggregates was confirmed by LTA (n = 4). Ns = not significant, *P < .05, **P < .01, scale bar 50 μm.

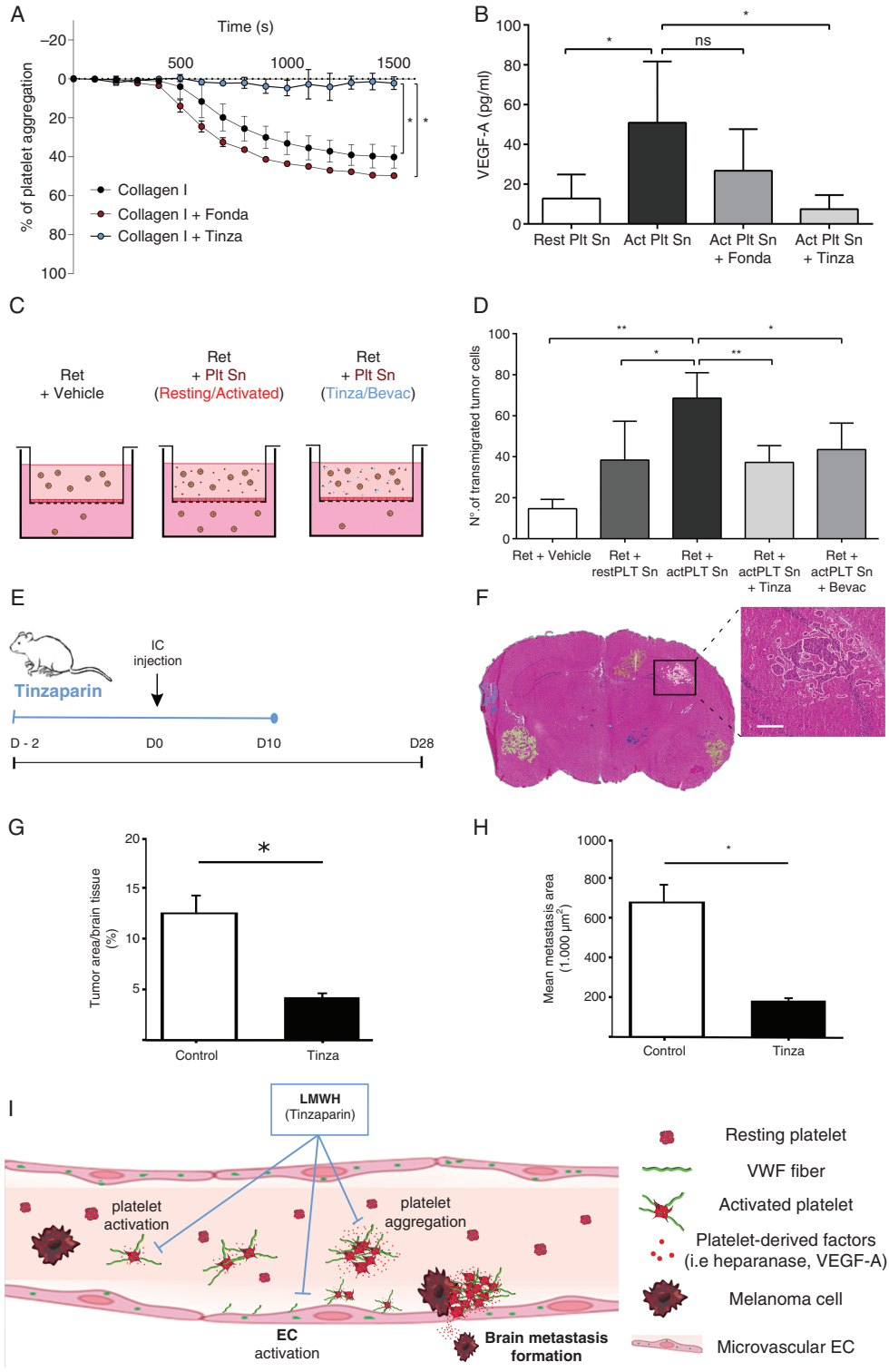

Figure 6. Tinzaparin reduces tumor cell transmigration and BM (A) The impact of tinzaparin (Tinza) and fondaparinux (Fonda) on collagen type I-mediated platelet activation was determined by LTA ($n = 4$). (B) Platelet releasates were analyzed by ELISA for VEGF-A secretion ($n = 3$ experiments). (C, D) Ret cell transmigration was analyzed using a transmigration assay ($n = 3$ experiments). (E) Intracardiac (IC) model: Anticoagulation with tinzaparin starts 2 days prior to heart injection of melanoma cells (A2058) and continues daily until day 10 and animals were euthanized on day 28. (F) H&E staining was performed to quantify the tumor load. Representative images show BMs and the area used to calculate the relative tumor area (G) and the mean metastasis area (H) in nontreated (Control) and tinzaparin-treated (Tinza) mice ($n \geq 3$ brains/group). (I) Schematic diagram showing VWF-mediated coagulation and BM formation. Ns = not significant, $^{*}P < .05$, $^{**}P < .01$, scale bar 200 µm.

of cancer patients.[52] Further, dalteparin did not improve overall survival of patients with lung cancer.[53] The discrepancies among the observations might be explained by the inclusion of different tumor types, cancer stages as well as differences in the applied anticoagulants. Compared to tinzaparin, fondaparinux and dalteparin are less efficient in blocking selectins and VEGF-A.[9,54,55] Tinzaparin is safe and efficacious in the treatment of venous thromboembolism in patients with cancer[56] demonstrating the need of clinical trials involving localized tumors without metastases to avoid the concept that LMWHs do not have an impact on survival and tumor progression.

Limitations of this study should be considered. One limitation is that although the combination of *in vitro*, *ex vivo*, and *in vivo* techniques allowed deep insights into the role of VWF in the brain metastatic cascade, it did not allow to dissect the role of platelet-derived VWF strings. To elucidate the specific contribution of platelet-derived VWF in the brain, bone marrow transplantations between WT and VWF-deficient mice could be applied. In addition, tinzaparin used to block coagulation and BM in this study makes it difficult to analyze the underlying mechanisms.

In conclusion, our data shed light on the biology of VWF at the BBB and expand our understanding of the pathophysiological mechanisms underlying thrombosis and the formation of BM in patients with malignant melanoma.

Supplementary Material

Supplementary material is available at *Neuro-Oncology Advances* online.

Keywords

melanoma | metastasis | platelets | thrombosis | von Willebrand factor

Funding

This work was funded by grants from the Deutsche Forschungsgemeinschaft (German Research Council), Germany (GRK2099 "Hallmarks of Skin Cancer"), the Deutsche Krebshilfe, Priority Program "Translational Oncology" #70112507, "Preventive strategies against BM", and the Erich und Gertrud Roggenbuck-Stiftung, Germany.

Acknowledgments

The authors thank Birgit Schneider for artwork.

Conflict of interest statement. The authors declare that the research was conducted in the absence of any commercial or financial relationships that could be construed as a potential conflict of interest. F.W. has received research funding from Roche, Genentech, Boehringer Ingelheim, and Divide & Conquer.

Authorship Statement. Study concept and design: J.R.R., M.J.F., F.W., A.T.B. Data analysis: C.G., C.M. Experiments: J.R.R., M.J.F., A.T.B., D.H., F.T.M., M.A.B., M.A., K.N., M.S.R., V.U., A.B., A.S., X.L., S.V., E.W. Patient sample collection: J.S. Data interpretation: J.R.R., M.J.F., F.W., K.P., S.W.S., A.T.B. Drafted manuscript: J.R.R., M.J.F., F.W., A.T.B. Approved final manuscript: all authors.

References

1. Berghoff AS, Rajky O, Winkler F, et al. Invasion patterns in brain metastases of solid cancers. *Neuro Oncol.* 2013;15(12):1664–1672.
2. Chamberlain MC, Baik CS, Gadi VK, Bhatia S, Chow LQ. Systemic therapy of brain metastases: non-small cell lung cancer, breast cancer, and melanoma. *Neuro Oncol.* 2017;19(1):i1–i24.
3. Valiente M, Ahluwalia MS, Boire A, et al. The evolving landscape of brain metastasis. *Trends Cancer.* 2018;4(3):176–196.
4. Alvarado G, Noor R, Bassett R, et al. Risk of intracranial hemorrhage with anticoagulation therapy in melanoma patients with brain metastases. *Melanoma Res.* 2012;22(4):310–315.
5. Andersen KK, Olsen TS. Risk of ischemic and hemorrhagic strokes in occult and manifest cancers. *Stroke.* 2018;49(7):1585–1592.
6. Schneider SW, Nuschele S, Wixforth A, et al. Shear-induced unfolding triggers adhesion of von Willebrand factor fibers. *Proc Natl Acad Sci USA.* 2007;104(19):7899–7903.
7. Obermeier HL, Riedl J, Ay C, et al. The role of ADAMTS-13 and von Willebrand factor in cancer patients: results from the Vienna Cancer and Thrombosis Study. *Res Pract Thromb Haemost.* 2019;3(3):503–514.
8. Huck V, Schneider MF, Gorzelanny C, Schneider SW. The various states of von Willebrand factor and their function in physiology and pathophysiology. *Thromb Haemost.* 2014;111(4):598–609.
9. Bauer AT, Suckau J, Frank K, et al. von Willebrand factor fibers promote cancer-associated platelet aggregation in malignant melanoma of mice and humans. *Blood.* 2015;125(20):3153–3163.
10. Goertz L, Schneider SW, Desch A, et al. Heparins that block VEGF-A-mediated von Willebrand factor fiber generation are potent inhibitors of hematogenous but not lymphatic metastasis. *Oncotarget.* 2016;7(42):68527–68545.
11. Feinauer MJ, Schneider SW, Berghoff AS, et al. Local blood coagulation drives cancer cell arrest and brain metastasis in a mouse model. *Blood.* 2021;137(9):1219–1232.
12. Zhao F, Falk C, Osen W, Kato M, Schadendorf D, Umansky V. Activation of p38 mitogen-activated protein kinase drives dendritic cells to become tolerogenic in ret transgenic mice spontaneously developing melanoma. *Clin Cancer Res.* 2009;15(13):4382–4390.
13. Kienast Y, von Baumgarten L, Fuhrmann M, et al. Real-time imaging reveals the single steps of brain metastasis formation. *Nat Med.* 2010;16(1):116–122.

14. Grässle S, Huck V, Pappelbaum KI, et al. von Willebrand factor directly interacts with DNA from neutrophil extracellular traps. *Arterioscler Thromb Vasc Biol.* 2014;34(7):1382–1389.
15. Yamamoto K, de Waard V, Fearns C, Loskutoff DJ. Tissue distribution and regulation of murine von Willebrand factor gene expression in vivo. *Blood.* 1998;92(8):2791–2801.
16. Mammadova-Bach E, Ollivier V, Loyau S, et al. Platelet glycoprotein VI binds to polymerized fibrin and promotes thrombin generation. *Blood.* 2015;126(5):683–691.
17. Gerotziafas GT, Petropoulou AD, Verdy E, Samama MM, Elalamy I. Effect of the anti-factor Xa and anti-factor IIa activities of low-molecular-weight heparins upon the phases of thrombin generation. *J Thromb Haemost.* 2007;5(5):955–962.
18. Rider CC, Mulloy B. Heparin, heparan sulphate and the TGF-beta cytokine superfamily. *Molecules.* 2017;22(5).
19. Noubade R, del Rio R, McElvany B, et al. von-Willebrand factor influences blood brain barrier permeability and brain inflammation in experimental allergic encephalomyelitis. *Am J Pathol.* 2008;173(3):892–900.
20. Suidan GL, Brill A, De Meyer SF, et al. Endothelial Von Willebrand factor promotes blood-brain barrier flexibility and provides protection from hypoxia and seizures in mice. *Arterioscler Thromb Vasc Biol.* 2013;33(9):2112–2120.
21. Kleinschnitz C, De Meyer SF, Schwarz T, et al. Deficiency of von Willebrand factor protects mice from ischemic stroke. *Blood.* 2009;113(15):3600–3603.
22. Zhao BQ, Chauhan AK, Canault M, et al. von Willebrand factor-cleaving protease ADAMTS13 reduces ischemic brain injury in experimental stroke. *Blood.* 2009;114(15):3329–3334.
23. Xu H, Cao Y, Yang X, et al. ADAMTS13 controls vascular remodeling by modifying VWF reactivity during stroke recovery. *Blood.* 2017;130(1):11–22.
24. O'Regan N, Gegenbauer K, O'Sullivan JM, et al. A novel role for von Willebrand factor in the pathogenesis of experimental cerebral malaria. *Blood.* 2016;127(9):1192–1201.
25. Petri B, Broermann A, Li H, et al. von Willebrand factor promotes leukocyte extravasation. *Blood.* 2010;116(22):4712–4719.
26. Doddapattar P, Dhanesha N, Chorawala MR, et al. Endothelial cell-derived von Willebrand factor, but not platelet-derived, promotes atherosclerosis in apolipoprotein e-deficient mice. *Arterioscler Thromb Vasc Biol.* 2018;38(3):520–528.
27. Verhenne S, Denorme F, Libbrecht S, et al. Platelet-derived VWF is not essential for normal thrombosis and hemostasis but fosters ischemic stroke injury in mice. *Blood.* 2015;126(14):1715–1722.
28. Deppermann C, Kraft P, Volz J, et al. Platelet secretion is crucial to prevent bleeding in the ischemic brain but not in the inflamed skin or lung in mice. *Blood.* 2017;129(12):1702–1706.
29. Macdonald JA, Murugesan N, Pachter JS. Endothelial cell heterogeneity of blood-brain barrier gene expression along the cerebral microvasculature. *J Neurosci Res.* 2010;88(7):1457–1474.
30. Fisher MJ. Brain regulation of thrombosis and hemostasis: from theory to practice. *Stroke.* 2013;44(11):3275–3285.
31. Franchini M, Frattini F, Crestani S, Bonfanti C, Lippi G. von Willebrand factor and cancer: a renewed interest. *Thromb Res.* 2013;131(4):290–292.
32. Böhm M, Gerlach R, Beecken WD, Scheuer T, Stier-Brück I, Scharrer I. ADAMTS-13 activity in patients with brain and prostate tumors is mildly reduced, but not correlated to stage of malignancy and metastasis. *Thromb Res.* 2003;111(1-2):33–37.
33. Mannucci PM, Canciani MT, Forza I, Lussana F, Lattuada A, Rossi E. Changes in health and disease of the metalloprotease that cleaves von Willebrand factor. *Blood.* 2001;98(9):2730–2735.
34. Dong JF, Moake JL, Nolasco L, et al. ADAMTS-13 rapidly cleaves newly secreted ultralarge von Willebrand factor multimers on the endothelial surface under flowing conditions. *Blood.* 2002;100(12):4033–4039.
35. Coppo P, Schwarzinger M, Buffet M, et al.; French Reference Center for Thrombotic Microangiopathies. Predictive features of severe acquired ADAMTS13 deficiency in idiopathic thrombotic microangiopathies: the French TMA reference center experience. *PLoS One.* 2010;5(4):e10208.
36. McGrath RT, van den Biggelaar M, Byrne B, et al. Altered glycosylation of platelet-derived von Willebrand factor confers resistance to ADAMTS13 proteolysis. *Blood.* 2013;122(25):4107–4110.
37. Fernandez MF, Ginsberg MH, Ruggeri ZM, Batlle FJ, Zimmerman TS. Multimeric structure of platelet factor VIII/von Willebrand factor: the presence of larger multimers and their reassociation with thrombin-stimulated platelets. *Blood.* 1982;60(5):1132–1138.
38. Kanaji S, Fahs SA, Shi Q, Haberichter SL, Montgomery RR. Contribution of platelet vs. endothelial VWF to platelet adhesion and hemostasis. *J Thromb Haemost.* 2012;10(8):1646–1652.
39. Dayananda KM, Singh I, Mondal N, Neelamegham S. von Willebrand factor self-association on platelet Gplbalpha under hydrodynamic shear: effect on shear-induced platelet activation. *Blood.* 2010;116(19):3990–3998.
40. Salven P, Heikkilä P, Joensuu H. Enhanced expression of vascular endothelial growth factor in metastatic melanoma. *Br J Cancer.* 1997;76(7):930–934.
41. Ascierto PA, Leonardi E, Ottaiano A, Napolitano M, Scala S, Castello G. Prognostic value of serum VEGF in melanoma patients: a pilot study. *Anticancer Res.* 2004;24(6):4255–4258.
42. Corrie PG, Marshall A, Nathan PD, et al. Adjuvant bevacizumab for melanoma patients at high risk of recurrence: survival analysis of the AVAST-M trial. *Ann Oncol.* 2019;30(12):2013–2014.
43. Küsters B, Leenders WP, Wesseling P, et al. Vascular endothelial growth factor-A(165) induces progression of melanoma brain metastases without induction of sprouting angiogenesis. *Cancer Res.* 2002;62(2):341–345.
44. Yano S, Shinohara H, Herbst RS, et al. Expression of vascular endothelial growth factor is necessary but not sufficient for production and growth of brain metastasis. *Cancer Res.* 2000;60(17):4959–4967.
45. Küsters B, Kats G, Roodink I, et al. Micronodular transformation as a novel mechanism of VEGF-A-induced metastasis. *Oncogene.* 2007;26(39):5808–5815.
46. Weis S, Cui J, Barnes L, Cheresh D. Endothelial barrier disruption by VEGF-mediated Src activity potentiates tumor cell extravasation and metastasis. *J Cell Biol.* 2004;167(2):223–229.
47. Fecci PE, Champion CD, Hoj J, et al. The evolving modern management of brain metastasis. *Clin Cancer Res.* 2019;25(22):6570–6580.
48. Strilic B, Offermanns S. Intravascular survival and extravasation of tumor cells. *Cancer Cell.* 2017;32(3):282–293.
49. Kircher DA, Silvis MR, Cho JH, Holmen SL. Melanoma brain metastasis: mechanisms, models, and medicine. *Int J Mol Sci.* 2016;17(9):1468.
50. Borsig L. Antimetastatic activities of heparins and modified heparins. Experimental evidence. *Thromb Res.* 2010;125(suppl 2):S66–S71.
51. Klerk CP, Smorenburg SM, Otten HM, et al. The effect of low molecular weight heparin on survival in patients with advanced malignancy. *J Clin Oncol.* 2005;23(10):2130–2135.
52. Kakkar AK, Levine MN, Kadziola Z, et al. Low molecular weight heparin, therapy with dalteparin, and survival in advanced cancer: the Fragmin Advanced Malignancy Outcome Study (FAMOUS). *J Clin Oncol.* 2004;22(10):1944–1948.

53. Macbeth F, Noble S, Evans J, et al. Randomized phase III trial of standard therapy plus low molecular weight heparin in patients with lung cancer: FRAGMATIC Trial. *J Clin Oncol*. 2016;34(5):488–494.

54. Stevenson JL, Choi SH, Varki A. Differential metastasis inhibition by clinically relevant levels of heparins–correlation with selectin inhibition, not antithrombotic activity. *Clin Cancer Res*. 2005;11(19 Pt 1):7003–7011.

55. Norrby K, Nordenhem A. Dalteparin, a low-molecular-weight heparin, promotes angiogenesis mediated by heparin-binding VEGF-A in vivo. *APMIS*. 2010;118(12):949–957.

56. Auer R, Scheer A, Wells PS, et al. The use of extended perioperative low molecular weight heparin (tinzaparin) to improve disease-free survival following surgical resection of colon cancer: a pilot randomized controlled trial. *Blood Coagul. Fibrinolysis*. 2011;22(8):760–762.